Plasma Chem Plasma Process (2017) 37:1223–1235
DOI 10.1007/s11090-017-9810-1

ORIGINAL PAPER

Evaluation of the Effect of Plasma Treatment Frequency on the Activation of Polymer Particles

Hisham M. Abourayana[1] · Vladimir Milosavljević[2,3] · Peter Dobbyn[1] · Denis P. Dowling[1]

Received: 25 December 2016 / Accepted: 6 March 2017 / Published online: 23 March 2017

Abstract This study investigates the influence of treatment frequency (1–150 kHz) on the atmospheric plasma activation of both silicone and polyethylene terephthalate (PET) particles. These polymer particles with diameters in the range 3–5 mm, were treated using either helium or helium/oxygen gas mixtures, in a barrel atmospheric plasma system. The level of polymer particles activation was monitored using water contact angle measurements. The effect of plasma treatment frequency on barrel heating was monitored using an infrared thermographic camera, the maximum barrel temperature after 15 min treatment was found to be 98 °C at a frequency of 130 kHz. Optical emission spectroscopy was used as a diagnostic tool to monitor changes in atomic and molecular species spectral intensity with experimental conditions, as well as a change in electron energy distribution function. Electrical characterisation studies demonstrated an increase in plasma power with increasing frequency, in the range investigated. X-ray photoelectron spectroscopy analysis indicate an increase of oxygen content on polymer surfaces after plasma treatment. For silicone particles, the minimum polymer water contact angle was obtained by using a frequency of 130 kHz. After 15 min treatment time, the water contact angle decreased from 141° to 11°. While for PET particles the optimum treatment frequency was found to be 70 kHz, resulting in a water contact angle decreased from 94° to 32°. This lower frequency was used due to the partial melting of the PET (Tg of 80 °C), when treated at the higher frequency.

Keywords Atmospheric plasma · Barrel reactor · Surface activation · Frequency

✉ Denis P. Dowling
denis.dowling@ucd.ie

[1] School of Mechanical and Materials Engineering, University College Dublin, Belfield, Dublin 4, Ireland

[2] BioPlasma Research Group, Dublin Institute of Technology, Dublin 1, Ireland

[3] Faculty of Physics, University of Belgrade, Belgrade, Serbia

Introduction

Plasma treatments are widely used to enhance the surface energy of polymers, particularly by the incorporation of polar groups [1, 2]. Polymers are however often processed as powders, for examples with applications in the textile industry, for hot-melt adhesives, filling for composite materials, 3D printing, and biotechnology [3]. Amongst the plasma reactor designs for the treatment of polymer particles are fluidized bed reactors, downer reactors and batch reactors [4–6]. Of these the most widely reported has been the fluidized bed system, it however has a difficulty in controlling the agitation of fluidized particles where there is a significant weight variation between the particles being treated [7]. An alternative is the use of a barrel reactor in which the particles are rotated and thus continually fall through the plasma zone. The plasma treatments are generally carried out using noble gases, e.g. He or Ar, with the addition of oxidizing gases e.g. air, CO_2 or O_2 [8, 9]. As with the treatment of polymer sheet material it is important to prevent thermal damage to the polymer particles during plasma activation. The level of polymer activation generally increases with the applied power to the plasma, however this increase in power is also associated with an increase in temperature [10].

Several studies have reported on the use of plasmas for the activation of polymer powders. Most of these studies focused on the development of the plasma reactors used for the treatment [11, 12], or on the effect of plasma parameters on the powder treatment such as treatment time and processing gas [13]. To the authors knowledge however, no study investigated the effect of plasma treatment frequency on the level of activation of the polymer particles. This type of investigation has however been carried out previously in the use of atmospheric plasma jets for killing bacteria [14]. It was established discharge frequency did indeed influence coupling efficiency and thus bacterial killing efficiency.

In this study the effect of systematically altering the plasma treatment frequency on polymer particle [silicone and polyethylene terephthalate (PET)] activation is investigated. In addition, the effect of frequency on discharge emission spectra, current and voltage as well as the heat generated in the treatment chamber were also studied.

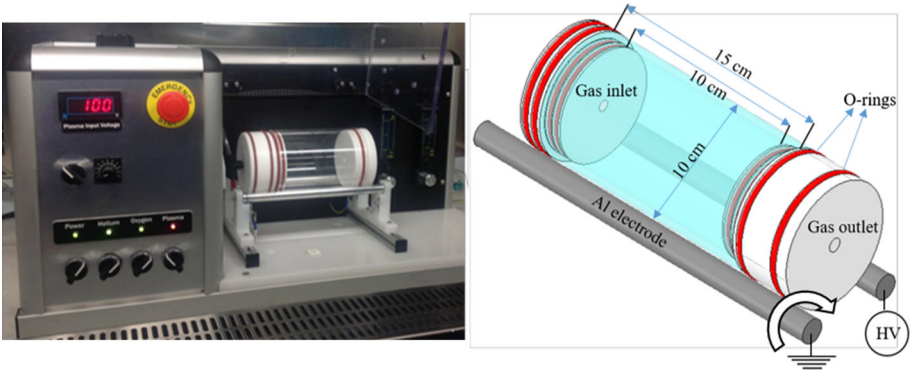

Fig. 1 Photograph of the barrel reactor (*left*) and schematic diagram of the barrel showing the combined roller/electrode arrangement which is in direct contact with the barrel (*right*)

Experimental

The barrel reactor [15] was designed and constructed as shown in Fig. 1. It consists of a quartz chamber with dimensions of 15 cm in length and 10 cm inner diameter. The chamber was sealed with two removable Teflon plugs, which were inserted 2.5 cm into the chamber, thus the effective treatment length was 10 cm. The plasma operated using a high voltage power generator (G2000 Redline technologies), with a frequency from 0 up to 500 kHz and input voltage of up to 300 V. Helium and helium/oxygen gas mixtures were used as processing gases. Their flow rates were 10 slm for helium and in the range of 0.01–0.03 slm for oxygen, these were controlled using rotameters (Bronkhorst). The plasma chamber was purged using helium gas at a flow rate of 10 slm, for 2 min before the plasma was ignited in order to remove the residual air. In this design, the plasma was generated between two aluminium rods, which are also used to rotate the chamber. These rods act as the biased and earthed electrodes. The powder charge of 20 g was agitated by rotation of the glass chamber, with a speed of approximately 7 rotations per minute.

A number of different techniques were used to monitor the barrel reactor. The applied voltage was measured using a North Star PVM-5 high voltage probe with a ratio of (1 V per kV), which was directly connected to the electrodes of the plasma barrel. The current measurements were obtained with a Bergoz Instrumentation France, toroidal current transformer (CT-E5.0) with an output of 5 V per Ampere. The current and voltage waveforms were monitored using a 4 channel digitizer (300 MHz bandwidth) Oscilloscope (Techtronix). Optical emission spectra of the plasma were obtained using an Ocean Optics USB4000 UV/VIS spectrometer with sensitivity in the 200–850 nm region, and with a resolution of approx. 1.2 nm. Light from the plasma passes through a focusing lens and a 2 m-long 400 μm multi-mode fibre optic cable were mounted directly under the most intense plasma region (between the two barrel electrodes). This optical emission spectroscopy (OES) technique is based on the integration of measured signals over a line-of-sight observation. Experiments were carried out to investigate species spectral intensities with varying frequencies voltage, and processing time. The latter time sequence of the recorded spectrum, was every 10 s for a duration of 1 min using an integration time of 2 s.

The temperature of the quartz wall of the plasma chamber was measured using a VarioCam high resolution infrared thermographic camera, with resolution of 640 × 480 pixels. Thermal measurements were obtained of the barrel wall after 15 min of plasma generation under different plasma operating frequencies.

The atmospheric plasma treatment of the silicone polymer and PET was investigated. The cylindrical silicone polymer particles had typical dimensions of 5.0 mm diameter and 0.5 mm thick were manufacturing from its precursors as described previously [16]. The PET was manufactured as a sheet material by Holfeld Plastics, Ireland and was cut into particulate samples with dimensions of approximately 3 × 4 × 0.35 mm. A Dataphysics Instruments OCA 20 Video Based Contact Angle Device, which utilises the sessile drop technique, was used to obtain water contact angles at room temperature. 0.5 μl drops were allowed to sit on the surface for 5 s (approx.) before water contact angles were measured. This was carried out both immediately after plasma treatment and at varying times after treatment, in order to determine the rate of hydrophobic recovery. Measurements were taken from at least 25 particles selected randomly (one measurement per particle) for each batch. The average of these measurements is then quoted as the contact angle. Polymer surface chemistry changes were monitored using X-ray photon electron spectroscopy (XPS) analysis (Kratos Analytical Axis Ultra system) set-up with a monochromated Al Kα

X-ray source. The measurements were obtained within 2 h of plasma activation of the polymers. The intensities of the peaks were determined as the integrated peak areas assuming the background to be linear. The thermal properties of the PET and silicone were determined using a differential thermal analysis system NETZSCH DSC 200F3 240-20-0863-L. At a heating rate of 10 °C/min. The glass transition temperature (Tg) for the two polymers was 80 and 440 °C respectively.

Results and Discussion

This discussion is divided into two sections, firstly the effect of the barrel plasma's treatment frequency on both the current and voltage, the intensity of the discharge species (by OES), as well as the temperature generated in the barrel are detailed. The effect of altering the treatment frequency on the level of polymer particle activation is then discussed.

Electrical Characterisation

The impact of operating frequency on the plasma power generated was investigated. In this study the root means square (RMS) of the voltage (V_{rms}) and current (I_{rms}) waveforms were obtained over a time period of approximately 0.1 ms. This procedure yields an estimation of the average AC power (P), namely (P = IV) of the non-sinusoidal waveforms according to Eq. 1 [17].

$$P_{average}(W) = V_{rms}\ (Volt) \times I_{rms}\ (Ampere) \tag{1}$$

For these experiments, the frequency was kept at a constant level during each treatment. The helium gas flow rate was fixed as 10 slm and operating voltage was fixed on 240 V. As shown in Fig. 2, it was found that the power generally increased with increasing frequency and the maximum output power obtained is 227 W at 130 kHz. A probable explanation for this increase in power with frequency is that the discharge current also increases and thus the plasma density [18].

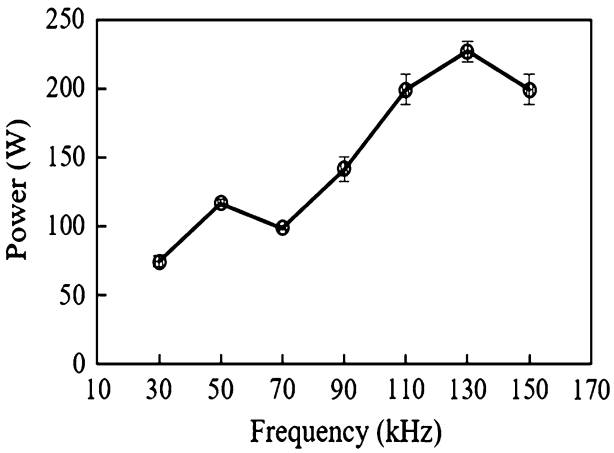

Fig. 2 Effect of frequency on the barrel plasma power. (He flow rate 10 slm and operating voltage 240 V)

The effect of oxygen flow rate on the helium plasma power was also investigated. As shown in Fig. 3 at a fixed frequency of 130 kHz, it was found that the power decreased with increasing oxygen flow rate due to partial discharge quenching (oxygen is an electronegative gas) [19].

Optical Emission Spectroscopy and Thermal Measurements

Optical emission spectra were obtained of both the He and He/O_2 plasmas in the spectral range from 250 to 850 nm in terms of identifying the reactive plasma species. The OES lens was centrally placed underneath the chamber between the high voltage and ground electrodes. The typical emission spectra of the helium plasma operating at 240 volts and 130 kHz are shown in Fig. 4. In the UV emission band, OH radicals OH $[A^2\Sigma^+ - X^2\Pi]$ around 307 nm are found [20]. The emission of the second positive system of molecular nitrogen N_2 $[C^3\Pi^+u - B^3\Pi^+g]$ with band heads, $\nu = 0 \rightarrow 0$, 1 are located at the wavelengths, $\lambda = 337$ and 358 nm are recorded. At $\lambda = 391$ nm the $\nu = 0 \rightarrow 0$ band of

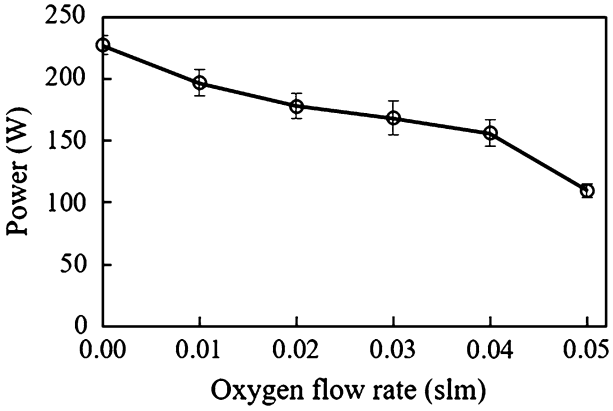

Fig. 3 Effect of oxygen flow rate on the barrel plasma power. (Helium flow rate 10 slm, operating voltage 240 V and frequency 130 kHz)

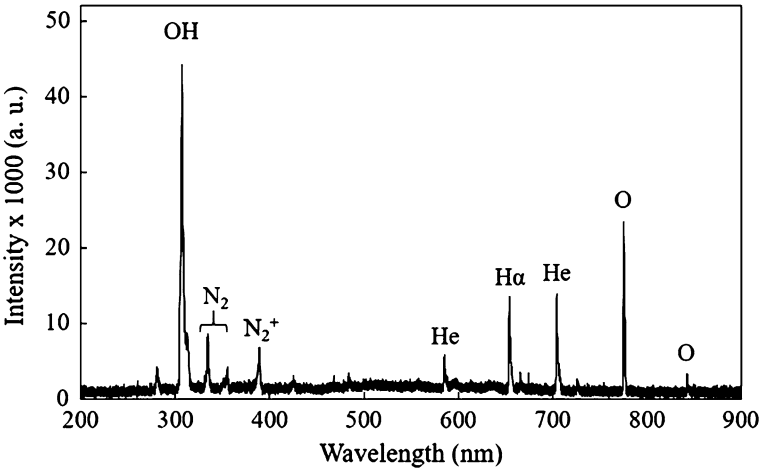

Fig. 4 Optical emission spectrum obtained from a He discharge formed in the barrel reactor

the first negative system of molecular nitrogen ions N_2^+ [$B^2\Sigma_u^+ - X^2\Sigma_g^+$] is observed [21]. Atomic hydrogen Hα transition (2p-3d) is recorded at $\lambda = 656$ nm [22]. For the pure helium discharge, the observation of emissions from OH, N_2 and N_2^+ is induced mainly by the air impurities diffused into the helium gas stream from open air [23]. The intensity of helium was monitored over four prominent atomic helium spectral lines. There are two spectral lines from the helium triplet spectra: He587 ($2p^3P^\circ_{1,2} - 3d^3D_{1,2,3}$) at 587 nm and He706 [$2p^3P^\circ_{1,2} - 3s^3S_1$] at 706 nm. There are also two spectral lines from the helium singlet spectra: He667 ($2p^1P^\circ_1 - 3d^1D_2$) at 667 nm and He728 ($2p^1P^\circ_1 - 3s^1S_0$) at 728 nm [24]. Helium's high metastable energy levels, which act as a "reservoir of energy", make it ideal for use for plasma processing [25]. The atomic oxygen triplet spectra O777 ($3s^5S^\circ_2 - 3p^5P_{1,2,3}$) and O844 ($3s^3S^\circ_1 - 3p^3P_{1,2,3}$) are also recorded near infrared region at $\lambda = 777$ and 844 nm respectively [26]. Oxygen could come from the ambient air, the He-O_2 gas mixture or from H_2O dissociation [24].

The effect of the treatment frequency and applied voltage on the resulting plasma species line intensity was investigated. To provide an indication of the relative importance of specific species to plasma processing conditions, the spectral intensity of a number of the OES peaks were integrated. Six wavelengths were selected for this investigation; 307 nm (OH307), 337 nm ($N_2$337), 391 nm (N_2^+391), 706 nm (He706), 777 nm (O777) and 656 nm (H656). The maximum intensity obtained by using frequency of 130 kHz and operating voltage of 340 V. It has been hard to find comparative study results for various driving frequency ranges. Most of the studies have inclined towards the application itself, paying less attention to the fundamental plasma characteristics [27]. Addition of small amount of oxygen to the helium plasma results in an increase in the intensity of singlet oxygen lines at 777 and 844 nm, while the intensity of the other emission lines has decreased. Oxygen is an electronegative gas, hence, addition of oxygen to the plasma produces O^- and O_2^- ions by electron attachment mechanisms, which results in a decrease of electron density and consequently decrease in the intensity of the other lines at a constant power [22]. Figure 5 shows the effect of frequency and oxygen flow rate on the plasma species.

Excited species of N_2(337) can be partly generated by energy transfer from helium metastable, in addition to the electron excitation [28, 29]. The ratio of second positive system N_2(337) and that of an ionized molecule N_2^+(391) (first negative system), are used to determine the plasma field strength and electron energy distribution function (EEDF) [30]. One of the main source of N_2^+(391) spectral emission, is a direct electron excitation

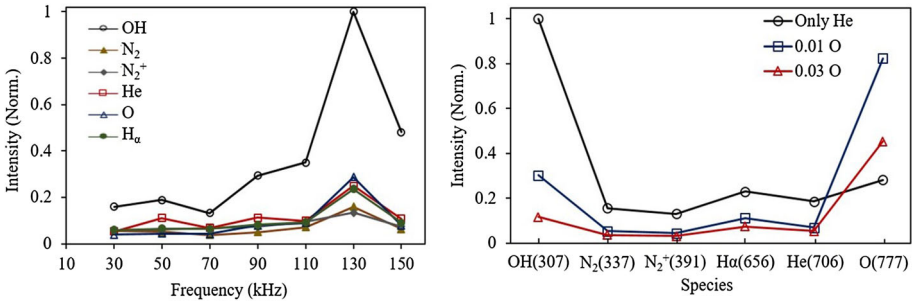

Fig. 5 Effect of frequency (*left*) and oxygen flow rate (*right*) on the plasma species intensities obtained by OES

from the ground level. However, this is not the only route. It is also possible to obtain this species due to the resonant excitation reaction of the He2 3s metastable with the ground state of N_2 [24]. The relative populations of the two vibronic levels, measured by emission spectroscopy, are related to the EEDF, in particular to the EEDF at energies above 11.03 eV, the threshold for the process. A change in the ratio between $N_2(337)$ and $N_2^+(391)$ spectral emissions indicates the change in the EEDF [31]. Namely, the shift in the nitrogen emissions from $N_2(337)$ to $N_2^+(391)$, this presumably occurs because of changes in the electron energy distribution. In particular, dissociative recombination with molecular ions rapidly removes low-energy electrons, such that the low-energy portion of the electron energy distribution is depressed when nitrogen is mixed with other molecules. Figure 6 shows the effect of frequency on the intensity ratio of $N_2(337)$ and $N_2^+(391)$. It indicates that altering the frequency used to generate the discharge leads to a change in the EEDF.

In order to obtain information on the temperature generated by the discharge at different frequencies, the temperature of the glass chamber was recorded 15 min after the plasma was ignited. As shown in Fig. 7 the temperature increased with increasing frequency. The maximum temperature obtained was 98 °C at a frequency of 130 kHz and 240 V operating voltage.

The effect of altering frequency on barrel temperature is clearly demonstrated in the thermographic images shown in Fig. 8. These show how the temperature obtained at the middle of the barrel is greater than that observed at the ends. The lower frequency discharge also appears to be more homogeneous based on these thermal images.

Plasma Treatment of Polymer Particles

A study was undertaken to evaluate the effect of processing conditions on polymer particle activation. Table 1 displays the plasma treatment conditions used in determining the optimum treatment conditions for the both silicone and PET particles. The helium flow rate and input voltage were maintained at 10 slm and 240 V respectively for all treatments.

For silicone particles, the effect of frequency and addition of oxygen to the helium discharge (10 slm) on the water contact angle of the polymer particles were investigated. As shown in Fig. 9 it was found that a small decrease in water contact angle was obtained by using a He only discharge after 2 min treatment time. The frequency was not found to

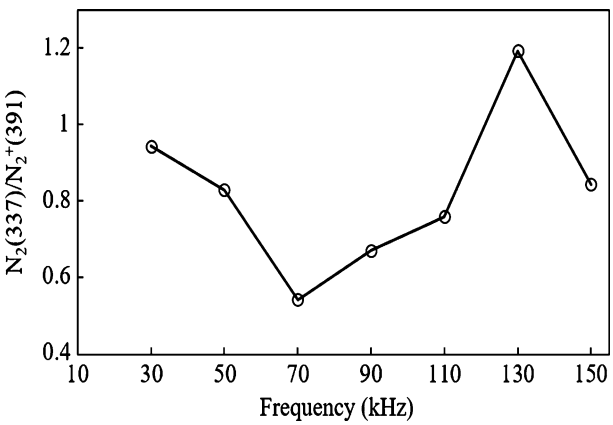

Fig. 6 Effect of frequency on the intensity ratio of $N_2(337)$ and $N_2^+(391)$

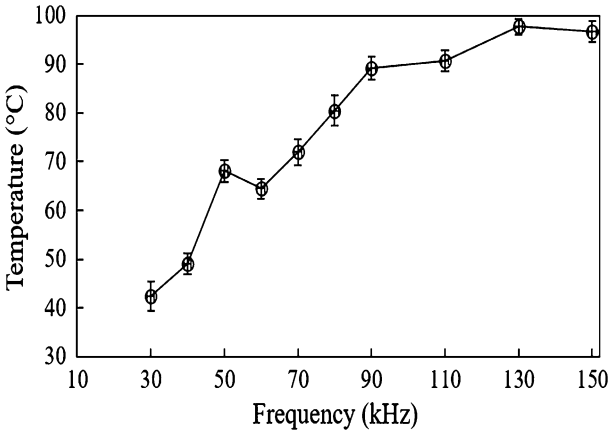

Fig. 7 Effect of plasma generating frequency on the barrel temperature

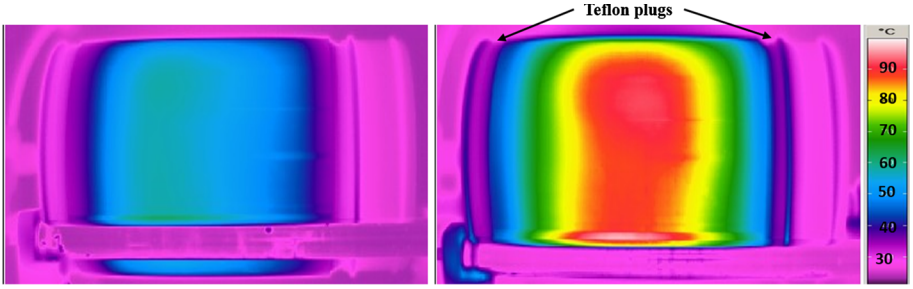

Fig. 8 Thermographic images of the barrel with plasma operating at a frequency of 70 kHz (*left*) and 130 kHz (*right*)

Table 1 Process parameters investigate for plasma treatment of silicone polymer and PET particles

	Frequency (kHz)	Treatment time (min)	O_2 flow rate (slm)
Silicone	30, 50, 70, 90, 110, 130 and 150	2, 5, 10 and 15	0.01, 0.02 and 0.03
PET	20, 30, 40, 50, 60, 70 and 80	2, 5, 10 and 15	0.01

have a significant effect on treated polymer particle water contact angle. In contrast the addition of oxygen into the helium plasma resulted in a decrease in water contact angle. The minimum water contact angle for silicone of 57° was obtained by using plasma frequency of 130 kHz and 0.02 oxygen flow rate. Comparing the 0.02 and 0.03 slm O_2 treatments, it is clear that there is increased plasma quenching with higher levels of oxygen addition, making the discharge significantly less effective at polymer activation. This is likely to be due to the quenching effect on OH, Hα and He metastables associated with the adding of oxygen into a helium plasma, as outlined earlier". This quenching effect has been reported previously by a number of authors [19, 32, 33].

The effect of treatment time on water contact angle of silicone particles was also investigated. As shown in Fig. 10, it was found that the water contact angle decreased with

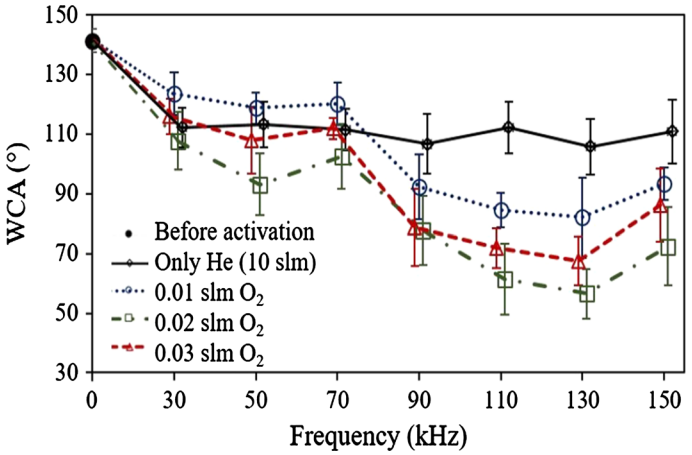

Fig. 9 Effect of plasma frequency and oxygen flow rate on the water contact angle of the silicone polymer particles. The 0.02 slm level of oxygen addition exhibits the highest level of activation. (He flow rate 10 slm and treatment time 2 min)

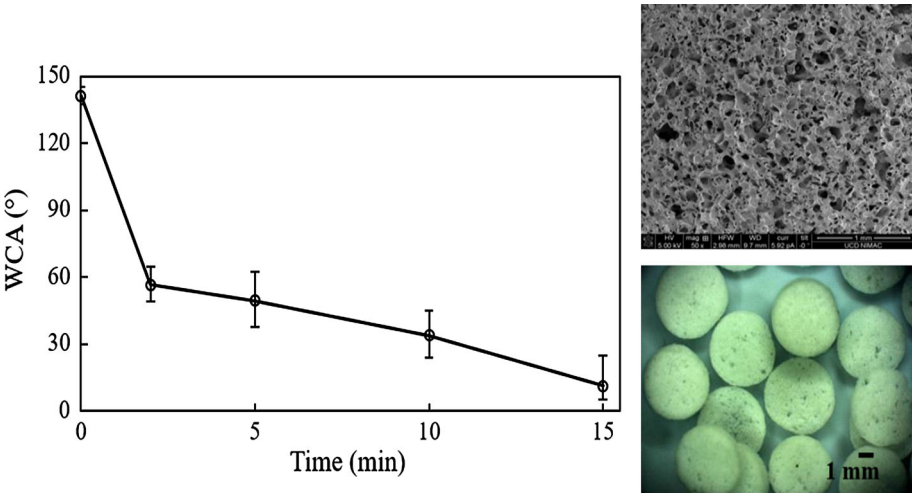

Fig. 10 Effect of plasma treatment time on the water contact angle of silicone polymers. (Frequency 130 kHz, He flow rate 10 slm and O_2 flow rate 0.02 slm). The photograph and SEM image (*right*) demonstrate the high surface roughness of the silicone particles

increasing treatment time and after 15 min the decrease obtained was from 141° to 11°. Optical microscopy examination of the treated particles indicated that no visual thermal damage was apparent as a result of the plasma treatments (Tg of silicone is 440 °C).

Figure 11 shows the effect of increasing the quantity (weight) of silicone particles on the water contact angle obtained after plasma activation. It was found that after 5 min treatment time, with increasing the particles weight from 20 to 30 g, there is a significant decrease in the activation effectiveness of the barrel plasma. Instead of a water contact angle reduction from 141° to 50°, only 89° was obtained using the 30 g load. Thus not

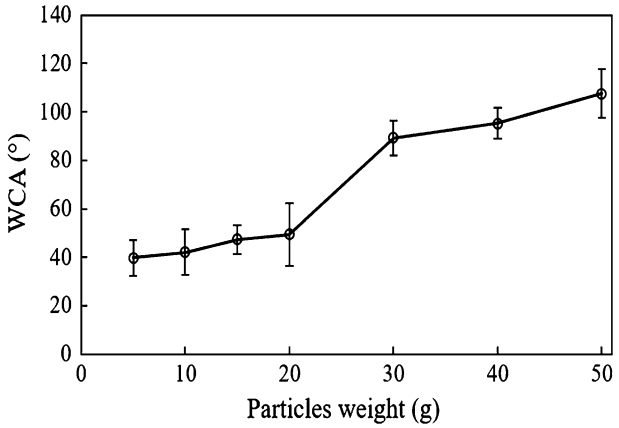

Fig. 11 Effect of increasing the weight of silicone particles on the water contact angle

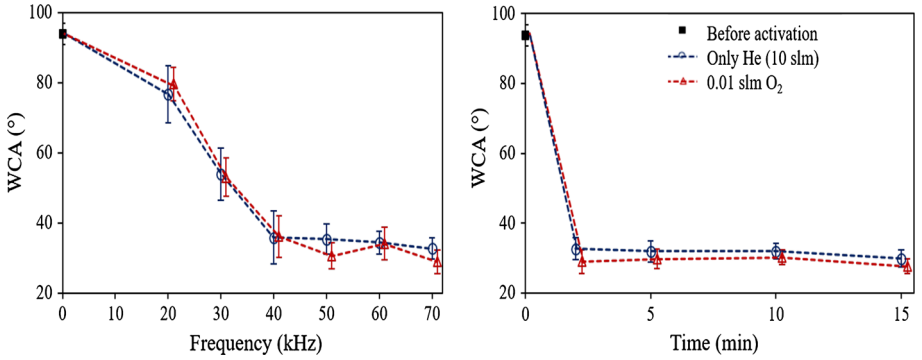

Fig. 12 Effect of plasma treatment frequency (*left*) and treatment time (*right*) on the water contact angle of the treated PET particles

unexpectedly as the larger quantity of particles due to their higher surface area require a longer plasma treatment time to yield the same contact angle.

The effect of treatment frequency on the water contact angle of PET particles was also investigated. This was limited to the investigation of frequencies in the range 0–70 kHz due to thermal damage to the polymer particles with treatments at higher frequencies (Tg of PET is 80 °C). As shown in Fig. 12, the optimum treatment frequency is in the range 40–70 kHz. There is no significant effect on water contact angle of PET particles with increasing treatment time above 2 min, or with the addition of 0.01 slm oxygen to the helium discharge. This is in contrast to the longer treatment times yielding improved wettability in the case of the silicone particles. The latter particles have a much rougher and porous morphology compared with that of the PET. This is likely to significantly increase their surface area, (as shown in Fig. 10) for this reason a longer treatment time is required for the silicone particles compared with that used for the activation of the PET particles.

The rate of hydrophobic recovery of the treated silicone and PET polymer particles was investigated after treatment at their optimized treatment frequencies of 130 and 70 kHz

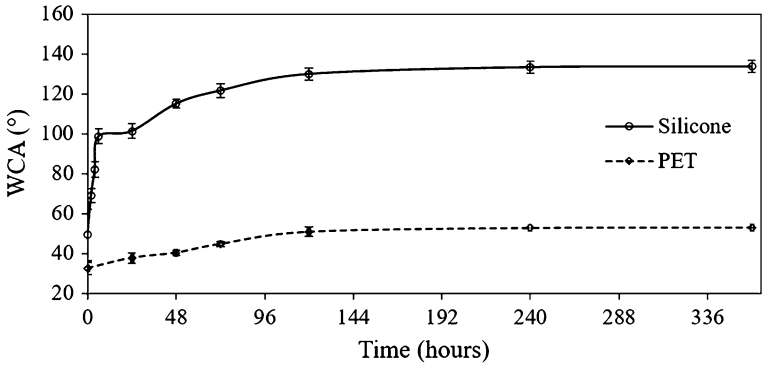

Fig. 13 Contact angle versus time for silicone and PET particles (frequency 130 kHz for silicone and 70 kHz for PET and treatment time 5 min)

Table 2 Atomic % of species on silicone and PET particles surface before and after plasma treatment

	% Si	% C	% O	C:O
Silicone				
Untreated	23.44	54.06	22.50	2.40
Plasma treated	25.71	33.04	41.25	0.80
PET				
Untreated		82.63	17.37	4.75
Plasma treated		73.32	26.68	2.74

respectively. After plasma treatment the polymer particles were stored in plastic vials and wrapped in aluminium foil to minimise surface contamination [34]. The hydrophobic recovery was examined at intervals for up to 15 days. In the case of silicone, the rate of hydrophobic recovery is more rapid as it returned to close to its unactivated contact angle value of 141° after approximately 100 h (Fig. 13). In contrast the PET water contact angle value plateaued at 51° after for the period from 100 to 360 h. This is significantly below the 94° obtained for the untreated polymer. The rate of hydrophobic recovery is dependent on the rate of reorientation of polar groups at the surface layer, the diffusion of unpolar groups from the sub-surface to the surface, and the reactions of free radicals at the surface [35, 36].

X-ray Photo Spectroscopy (XPS) Analysis

The surface chemistry changes associated with the plasma treatments of silicone and PET polymer particles was monitored by XPS. Table 2 shows the compositions of the silicone and PET polymers before and after plasma treatment. The C:O ratios for silicone and PET polymers before plasma treatment are 2.40 and 4.75 respectively. After plasma treatment the ratios were found to be decreased to 0.80 and 2.74 respectively. These results are consistent with results reported previously [15]. As expected plasma surface activation is largely associated with the incorporation of oxygen into the polymer surface, with the formation of oxygen-containing functionalities, such as Si–O onto silicone polymer surface and C–O and O–C=O onto PET surface [34, 37, 38].

Conclusions

This study investigated the effect of treatment frequency on the performance of a novel barrel plasma source for the plasma activation polymer particles. The treatments were carried out using both silicone and PET particles in He and He/O_2 discharges. Electrical characterisation indicated that the plasma power increased with increasing frequency and the maximum output power obtained is 227 W at 130 kHz. OES analysis demonstrated the increase in atomic species intensities with increased frequency, the maximum plasma species intensity was obtained by using frequency of 130 kHz. Addition of small amount of oxygen to the helium plasma results in an increase in the intensity of singlet oxygen lines, while the corresponding intensity of the other emission lines were decreased, due to partial quenching of the discharge. EEDF shows a strong dependence on the plasma generator frequencies, and a correlation with a spectral emission of the monitored plasma species. Thermal imaging analysis also demonstrated that the barrel temperature increased with increasing frequency and the maximum plasma temperature were obtained using a frequency of 130 kHz. The influence of plasma processing parameters such as frequency and treatment time on the level of surface activation, based on water contact angle (WCA) measurements was investigated. For silicone particles, the WCA decreased with increasing treatment time and the maximum reduction in WCA was achieved at 130 kHz, after a 15 min plasma treatment by using a flow rate 10 slm of He and 0.02 of oxygen. Further increasing the oxygen flow rate has a quenching effect on the discharge and thus its efficiency in activating the polymer surface. For PET, the WCA was reduced from 93° to 32° after 2 min treatment time. Increasing the frequency more than 70 kHz leads to thermal damage of the PET particles. This study concluded that treatment frequency, processing time and polymer particle type are critical parameters in deciding on the plasma activation conditions to be used with the barrel plasma system.

Acknowledgements This research is partially support by the Irish Centre for Composites Research (IComp).

References

1. Chen G, Chen S, Zhou M, Feng W, Gu W, Yang S (2006) J Phys D Appl Phys 39:5211–5215
2. Abourayana H, Dowling D (2015) In: Aliofkhazraei M (ed) Plasma processing for tailoring the surface properties of polymers. Intech, Rijeka
3. Pavlatova M, Horakova M, Hladik J, Spatenka P (2012) Acta Polytech 52:83–88
4. Vivien C, Wartelle C, Mutel B, Grimblot J (2002) Surf Interface Anal 34:575–579
5. Patra N, Hladik J, Pavlatova M, Militký J, Martinová L (2013) Polym Degrad Stab 98:1489–1494
6. Arpagaus C, Sonnenfeld A, Rudolf von Rohr P (2005) Chem Eng Technol 28:87–94
7. Kim J, Kim Y, Choi H (2002) Korean J Chem Eng 19:632–637
8. Claudia R, Ruggero B, Elena S, Giovanni M, Maria M, Bruno M, Giulio P (2003) Appl Surf Sci 211:386–397
9. Abou Rich S, Dufour T, Leroy P, Nittler L, Pireaux J, Reniers F (2014) J Phys D Appl Phys 47:065203
10. Donegan M, Milosavljevic V, Dowling D (2013) Plasma Chem Plasma Process 33:941–957
11. Arpagaus C, Rudolf von Rohr P, Rossi A (2005) Surf Coat Technol 200:525–528
12. Oberbossel G, Guntner A, Kundig L, Roth C, Rudolf von Rohr P (2015) Plasma Process Polym 12:285–292
13. Quitzau M, Wolter M, Kersten H (2009) Plasma Process Polym 6:S392–S396
14. Chebbi A, Sharkey M, Staunton C, McDonnell K, Dowling D (2015) Biointerphases 10:29507
15. Abourayana H, Milosavljevic V, Dobbyn P, Cullen P, Dowling D (2016) Surf Coat Technol 308:435–441

16. Abourayana H, Barry N, Dobbyn P, Dowling D (2015) J Min Metal Mater Eng 1:57–64
17. Nwankire C, Law V, Nindrayog A, Twomey B, Niemi K, Milosavljevic V, Graham W, Dowling D (2010) Plasma Chem Plasma Process 30:537–552
18. Jidenko N, Petit M, Borra J (2006) J Phys D Appl Phys 39:281–293
19. Milosavljević V, Ellingboe A, Daniels S (2011) Eur Phys J D 64:437–445
20. Laux C, Spence T, Kruger C, Zare R (2003) Plasma Sources Sci Technol 12:125–138
21. Machala Z, Janda M, Hensel K, Jedlovsky I, Lestinska L, Foltin V, Martisovits V, Morvova M (2007) J Mol Spectrosc 243:194–201
22. Thiyagarajan M, Sarani A, Nicula C (2013) J Appl Phys 113:233302
23. Xiong Q, Nikiforov A, González M, Leys C, Lu X (2013) Plasma Sources Sci Technol 22:15011
24. Milosavljevic V, Donegan M, Cullen P, Dowling D (2014) J Phys Soc Jpn 83:014501
25. Milosavljević V, Popović D, Ellingboe AR (2009) J Phys Soc Jpn 78:84501
26. Krstulović N, Labazan I, Milošević S, Cvelbar U, Vesel A, Mozetic M (2006) J Phys D Appl Phys 39:3799–3804
27. Kim D, Jung H, Gweon B, Moon S, Rhee J, Choe W (2011) Phys Plasmas 18:043503
28. Nascimento F, Moshkalev S, Machida M (2015) arXiv.org
29. Bibinov N, Fateev A, Wiesemann K (2001) J Phys D Appl Phys 34:1819–1826
30. Paris P, Aints M, Laan M, Valk F (2004) J Phys D Appl Phys 37:1179–1184
31. Paris P, Aints M, Valk F, Plank T, Haljaste A, Kozlov K, Wagner H (2005) J Phys D Appl Phys 38:3894–3899
32. Mohan J, Ramamoorthy A, Ivanković A, Dowliong D, Murphy N (2014) J Adhes 90:733–754
33. Twomey B, Nindrayog A, Niemi K, Graham W, Dowling D (2011) Plasma Chem Plasma Process 31:139–156
34. Williams R, Wilson D, Rhodes N (2004) Biomaterials 25:4659–4673
35. Yang S, Gupta M (2004) Surf Coat Technol 187:172–176
36. Jongsoo K, Chaudhury M, Owen M, Orbeck T (2001) J Colloid Interface Sci 244:200–207
37. Pandiyaraj K, Selvarajan V, Deshmukh R, Gao C (2009) Vacuum 83:332–339
38. Gonzalez E, Barankin M, Guschl P, Hicks R (2008) Langmuir 24:12636–12643